Pharm Res (2016) 33:2107–2116
DOI 10.1007/s11095-016-1949-6

RESEARCH PAPER

Biopharmaceutical Evaluation of Novel Cyclosporine A Nano-matrix Particles for Inhalation

Hideyuki Sato[1] • Hiroki Suzuki[1] • Keisuke Yakushiji[1] • Jennifer Wong[2] • Yoshiki Seto[1] • Robert K. Prud'homme[3] • Hak-Kim Chan[2] • Satomi Onoue[1]

Received: 4 March 2016 / Accepted: 13 May 2016 / Published online: 25 May 2016

ABSTRACT

Purpose This study was undertaken to evaluate the biopharmaceutical properties of cyclosporine A (CsA)-loaded nano-matrix particles for inhalation.

Methods Nano-matrix particles of CsA with mannitol (nCsAm) were prepared by a flash nano-precipitation technique employing a multi-inlet vortex mixer and evaluated in terms of physicochemical properties, anti-inflammatory effect in the rat model of airway inflammation, pharmacokinetic behavior, and distributions of CsA to side-effect-related organs after intratracheal administration.

Results In nCsAm, spherical nano-particles of CsA were covered with mannitol and the mean particle size was 1.3 μm. The *in vitro* Next Generation Impactor analysis demonstrated fine inhalation performance with a fine particle fraction value of 65.8%. Intratracheal nCsAm (100 μg-CsA/rat) significantly attenuated the recruitment of inflammatory cells into the airway in the rat model of airway inflammation, followed by suppression of the inflammatory biomarkers. After intratracheal nCsAm at a pharmacologically effective dose (100 μg-CsA/rat), there was a 42–47-fold decrease in the distribution of CsA to side-effect-related organs such as the kidney and liver compared with oral CsA at a toxic dose (10 mg-CsA/kg), potentially leading to avoidance of systemic side-effects of CsA.

Conclusion Upon these findings, nCsAm prepared with the flash nano-precipitation technique could be a novel dosage form of CsA for inhalation therapy of airway inflammation with a better safety margin.

KEY WORDS anti-inflammatory effect · cyclosporine A · inhalation · nano-matrix particles · pharmacokinetic control

ABBREVIATIONS

BALF	Bronchoalveolar lavage fluid
COPD	Chronic obstructive pulmonary disease
CsA	Cyclosporine A
DLS	Dynamic light scattering
DSC	Differential scanning calorimetry
FPF	Fine particle fraction
HPLC	High performance liquid chromatography
IL	Interleukin
MIVM	Multi inlet vortex mixer
MPO	Myeloperoxidase
nCsAm	Nano-matrix CsA particles with mannitol
NGI	Next generation impactor
OVA	Ovalbumin
PXRD	Powder X-ray diffraction
SEM	Scanning electron microscopy

INTRODUCTION

Cyclosporine A (CsA) has been widely used for the prevention of allograft rejection in various organ transplantations and the treatment of autoimmune diseases owing to its inhibition of various T-lymphocyte functions, especially the production of interleukin-2 (IL-2) (1–3). The orally-dosed CsA could be a promising dosage option for the treatment of lung transplant

✉ Hak-Kim Chan
kim.chan@sydney.edu.au

✉ Satomi Onoue
onoue@u-shizuoka-ken.ac.jp

[1] Department of Pharmacokinetics and Pharmacodynamics, School of Pharmaceutical Sciences, University of Shizuoka, 52-1 Yada, Suruga-ku, Shizuoka 422-8526, Japan

[2] Advanced Drug Delivery Group, Faculty of Pharmacy, The University of Sydney, Building A15, Sydney, NSW 2006, Australia

[3] Department of Chemical & Biological Engineering, Princeton University, A301 EQUAD, Princeton, New Jersey 08544, USA

patients who do not tolerate tacrolimus (4). There have been a number of reports on the application of CsA to the treatment of airway inflammation associated with asthma and chronic obstructive pulmonary disease (COPD) model animals, since T-cells can be key effector cells in the pathologies of these inflammatory diseases (5–7). In spite of the attractive therapeutic potential of CsA, the application of oral formulations to the treatment of respiratory diseases would be challenging due to the risk of high systemic exposure after oral administration and subsequent severe adverse side-effects including nephrotoxicity, hepatotoxicity, hypertension, and neurotoxicity (8,9). Lung-specific delivery of a sufficient amount of CsA can hardly be controlled by oral administration because of the high variability of oral bioavailability caused by its high molecular weight, high lipophilicity, and low intestinal permeability (10). Pulmonary administration would be a promising strategy for the treatment of respiratory diseases since it could deliver an efficacious drug level to the affected area and minimize systemic exposure of the drug after administration (11–13). A number of clinical trials have been carried out to evaluate the effects of inhaled CsA in lung transplant recipients (14,15), and the clinical application of inhaled CsA formulation has been desired for many years.

The dry powder inhaler (DPI) is the preferred delivery system for pulmonary drug administration since device is portable and compact, no propellant is required, and the ease of administration increase patient compliance (16). Although a DPI delivery system is desirable for the treatment of respiratory diseases, it would be challenging to achieve a particle design with desirable aerodynamic properties such as particle size, shape, flowability, and density to deposit efficiently from the trachea to the lung periphery (17). Even after reaching the respiratory tract, poorly water-soluble particles tend to be eliminated by innate mechanisms such as phagocytosis by alveolar macrophages and mucociliary clearance in the lung (18,19). A specific range of aerodynamic particle sizes (1–5 μm) is optimal for efficient pulmonary delivery of drug (20). Enhanced solubility of CsA could be a key consideration in avoiding clearance of the drug particles from the lung. Fine particles with a high specific surface area lead to improved solubility and dissolution; however, these small particles are generally cohesive, so they aggregate and demonstrate poor dispersibility of the powders. To overcome these drawbacks, a number of pharmaceutical technologies have been developed to achieve effective pulmonary delivery. DPI systems of CsA have been produced with wet-milling technique (7), spray-drying (21) and spray freeze-drying (22). Micron-sized aggregates of nano-particles defined as nano-matrix particles with desirable inhalation properties have been produced by the combination use of a nano-precipitation technique and spray-drying (23,24). In the previous report, the flash nano-precipitation method using a multi inlet vortex mixer (MIVM) was applied to the production of inhalable nano-matrix particles of CsA (nCsAm). The process was demonstrated to be rapid, precisely controlled, and scalable; and the particles produced had the required physicochemical properties for inhalation (24). These observations prompted us to evaluate the therapeutic potential and pharmacokinetic behavior of CsA after intratracheal administration of nCsAm.

The main purpose of the present study was to evaluate the biopharmaceutical properties of nCsAm as an inhalable formulation for the treatment of airway inflammation. In this study, nanoformulations of CsA with mannitol matrices, nCsAm were prepared by combination of the flash nano-precipitation technique and spray-drying. The physicochemical properties of the powder were characterized in terms of morphology, crystallinity, and *in vitro* inhalation. The anti-inflammatory effect of nCsAm was evaluated using an ovalbumin (OVA)-sensitized asthma/COPD animal model. The systemic exposure and tissue distributions of CsA in side-effect-related tissues such as the liver and kidney were also assessed to clarify the risk of side-effects after oral and intratracheal administration of CsA samples.

MATERIALS AND METHODS

Materials

CsA was purchased from Changzhou An-Yuan Import and Export Corporation (Changzhou, China); soy bean lecithin from Cargill Texturizing Solutions (Wayzata, USA); α-lactose monohydrate from Friesland Campina Domo (Amersfoort, Netherlands); Slipicone®, silicone release spray, from DC Products (Mount Waverly, Australia); and mannitol was kindly supplied by Pharmaxis (Frenchs Forest, Australia). All other chemicals were purchased from commercial sources.

Preparation of Nano-matrix CsA Particles

A nano-suspension of CsA was produced by the flash nano-precipitation method using a four-stream MIVM as reported previously (24). The mixer consisted of four inlets through which liquid reactants were pumped at controlled flow rates. Briefly, CsA was dissolved in absolute ethanol at a concentration of 50 mg/mL (Solution I). Lecithin and lactose were dissolved in water at 0.0125% *w/v* and 0.5% *w/v*, respectively (Solution II). Solution I was loaded into two syringes and solution II was also loaded into two other syringes at the same volume. All four syringes were connected to the MIVM with each dispensing 20 mL at 30 mL/min. Micro-mixing and nano-particle precipitation occurred inside the mixing chamber. The product was collected from the outlet into a beaker with 400 mL of deionized water stirred by a magnetic stirrer. Mannitol was put into the suspension with a mass loading equal to the CsA in the nanoparticles. The suspension was

refrigerated for at least 2 h and then spray-dried using a Büchi Mini Spray-Dryer B-290 (Büchi Labortechnik, Flawil, Switzerland) connected to a Büchi Dehumidifier B-296 (in open loop, blowing mode) under the following conditions: inlet temperature of 120°C, outlet temperatures of 70–89°C, aspiration rate of 100%, atomizing air flow at 819 NL/h and liquid feed rate of 3.5 mL/min. In all cases, the powder from the collector was transferred to separate sealed containers and stored with silica gel desiccant at 22°C until further analysis and processing.

Dynamic Light Scattering

The particle size of nano-particles prepared with MIVM was measured by dynamic light scattering (DLS) (Malvern Zetasiser Nano ZS, Malvern, Worcestershire, UK). The measurement parameters were as follows: the particle and dispersant refractive indices were 1.578 and 1.338, respectively. The absorption value of CsA was 0.1 and the dispersant viscosity was 1.367 mPa • s. The samples were measured in a disposable cuvette at 20°C in triplicate.

Scanning Electron Microscopy

The surface morphology of CsA samples was characterized by scanning electron microscopy (SEM) using a secondary detector at 5 kV (Zeiss Ultra Plus, Carl Zeiss SMT AG, Oberkochen, Germany). Prior to imaging, samples were dispersed onto sticky carbon tape, mounted on SEM stubs, and sputter coated with approximately 15 nm thick gold using a K550X sputter coater (Quorum Emitech, Kent, UK).

Laser Diffraction

The particle size distribution of nCsAm was determined by diffraction through a Scirocco 2000 dry powder feeder (Malvern Instruments, Worcestershire, UK). Samples of powder (approximately 10 mg) were dispersed in triplicate at 4 bar. Measurement parameters were as follows: obscuration of 0.3–10%, particle refractive index and absorption of 1.575 and 0.1, respectively; and the dispersant refractive index for air was 1.000. The data were expressed as D_{10}, D_{50}, and D_{90} which are the equivalent spherical volume diameters at 10, 50, and 90% cumulative volume, respectively. The span, which is the breadth of the particle size distribution, is defined as $(D_{90}–D_{10})/D_{50}$.

Differential Scanning Calorimetry and Powder X-ray Diffraction

Differential scanning calorimetry (DSC) thermograms of the CsA samples were obtained using a Model 823e DSC (Mettler Toledo, Canton, USA). Each sample (3 ± 1 mg) was heated from 20 to 400°C at a rate of 10°C/min under constant nitrogen purge. Powder X-ray diffraction (PXRD) patterns were recorded using an X-ray diffractometer (Model XRD-6000, Shimadzu Corporation, Kyoto, Japan) with Cu Kα radiation at 40 kV and 30 mA. The experiment was carried out under ambient conditions and the data were collected with angular increments of 0.02°/s per step covering a 2θ range of 5–40°.

Next Generation Impactor

The *in vitro* aerosol performance of nCsAm was characterized using a Next Generation Impactor (NGI) impactor (Copley Scientific, Nottingham, UK). Each impactor stage was sprayed with Slipicone® silicone prior to experiments to minimize particle bounce and re-entrainment, and the solvent was allowed to evaporate before the unit was re-assembled. An Aerolizer® (Novartis Australia Pty. Ltd., North Ryde, Australia) inhaler was loaded with an empty capsule and fitted with a rubber adapter to a calibrated flow meter (TSI 3063, TSI Instruments Ltd., Shoreview, USA) to check and adjust the total flow rate to 100 L/min. Samples of nCsAm (5 ± 0.2 mg) were manually filled into size 3 hydroxypropyl methylcellulose capsules (Capsugel, West Ryde, Australia). Each run dispersed one capsule using air drawn through the impactor at 100 L/min for 2.4 s, and was repeated in triplicate. After dispersion, drug that deposited on the device, capsule, adaptor, and each impactor stage were exhaustively washed with 5 mL of methanol/water solution (volumetric ratio 85:15) except for Stage 1 which was washed with 15 mL of the same solution. The CsA concentration was determined using high performance liquid chromatography (HPLC). The mobile phase consisted of acetonitrile, methanol, water, and phosphoric acid in 360/90/50/2.5% *v/v*. The HPLC system consisted of a SPD-20A UV–VIS detector (detection wavelength: 210 nm), LC-20AT pump, and SIL-20A HT Autosampler controlled by LC Solution software (Shimadzu Scientific Instruments, Kyoto, Japan). Samples were injected (50 µL) into an Altima® C18 5 µm 4.6 × 250 mm column (Alltech Associates, Deerfield, USA) at a flow rate of 1.5 mL/min (retention time of CsA: 7 min). The fine particle fraction (FPF) percentage was defined as the mass fraction <5 µm with respect to the recovered dose. This cumulative mass fraction was obtained by interpolation between the two cumulative mass fractions corresponding to the cutoff diameters for Stages 2 and 3 at 100 L/min.

Animals and Drug Inhalation

Male Sprague–Dawley rats (8–11 weeks of age; Japan SLC, Shizuoka, Japan) were housed three per cage in the laboratory with free access to food and water. The laboratory condition was maintained on a 12 h dark/light cycle in a room with

controlled temperature (24 ± 1°C) and humidity (55 ± 5%). Animals were fasted for 12 h before experiments. All procedures used in the present study were conducted according to the guidelines approved by the Institutional Animal Care and Ethical Committee of University of Shizuoka.

To induce the airway inflammation, sensitization and airway challenge with OVA were performed as described previously (25). The rats were sensitized on days 0 and 14 by intraperitoneal injection of 100 μg of OVA with 5 mg of aluminum hydroxide. After the last sensitization of OVA at 24 h, they were anesthetized with sodium pentobarbital (50 mg/kg, *i.p.*) and received an airway challenge by intratracheal administration of OVA respirable powder (100 μg-OVA/rat) using a Penn Century powder insufflation delivery device (DP-4, INA Research Inc., Nagano, Japan). At 1 h before the intratracheal sensitization, nCsAm (100 μg-CsA/rat) or vehicle (lactose powder) was administered via intratracheal insufflation. A bolus of air (2 mL) from an attached syringe was used to deliver the preloaded powder from the chamber of the insufflator into the rat airways. At 24 h after OVA challenge, rats were exsanguinated via the descending aorta under anesthesia with sodium pentobarbital (50 mg/kg, *i.p.*) to obtain the bronchoalveolar lavage fluid (BALF) and lung tissue.

Inflammatory Cells and Biomarkers in the BALF

To obtain the BALF, phosphate buffered saline (PBS) (5 mL) was infused into the lung and withdrawn through tracheal cannulation five times after exsanguination. BALF was pooled and immediately centrifuged at 112×*g* for 5 min. The supernatant was removed and the cells were resuspended with PBS (1 mL). The number of total cells in BALF was counted using an automated cell counter TC20 (Bio-Rad Laboratories Inc., Tokyo, Japan) after the addition of an equal amount of 0.2% trypan blue. The collected BALF samples were stained by the Wright–Giemsa stain method to identify the type of inflammatory cells. The supernatant obtained from BALF was stored at −20°C for biochemical analysis.

Enzymatic detection of myeloperoxidase (MPO) activity in BALF was performed according to the previous report with minor modifications (26). In brief, assay mixtures consisted of 40 μL H_2O_2 (final concentration 0.3 mM) in 80 mM sodium phosphate buffer (pH 5.4) and 50 μL BALF. The reaction was initiated by addition of 10 μL *3,3′,5,5′*-tetramethylbenzidine (final concentration 1.6 mM) in dimethyl sulfoxide at 37°C, and stopped after 2 min by the addition of 0.18 M H_2SO_4. After the reaction, optical density was determined at 450 nm by UV–VIS spectrophotometer.

Collagen Synthesis

The collagen content in the lung tissues was determined by Sircol collagen assay (Biocolor Ltd., Belfast, Northern Ireland, UK) in accordance with the manufacturer's instructions. The sircol collagen assay has been demonstrated to quantify the collagen content in biological tissues in previous studies (27). Briefly, the right middle lobe (ca. 0.2 g) of the lung was removed after BALF, and then the lung was homogenized in 1 mL of PBS and centrifuged (10,000×*g*) for 10 min at 4°C. The pellets were washed with 1 mL of PBS and centrifuged (10,000×*g*) for 10 min at 4°C two times. Collagen was solubilized in 0.5 M acetic acid. Extracts were incubated with Sirius red dye and absorbance was measured at 540 nm using a microplate reader (Safire; Tecan, Mannedorf, Switzerland). The amount of collagen is expressed in units of μg/g of wet tissue.

Systemic Exposure of CsA After Intratracheal or Oral Administration

Blood samples (volume of 200 μL) were taken from the tail vein at the indicated times after oral administration of Neoral® (10 mg-CsA/kg) or intratracheal administration of nCsAm (100 μg-CsA/rat). The blood samples were centrifuged at 10,000×*g* to obtain plasma samples which were then kept frozen below −20°C until chemical analysis. The concentrations of CsA in plasma were determined by an internal standard method using UPLC/ESI-MS. Briefly, 100 μL of acetonitrile and 5 μL of internal standard (tamoxifen, 500 ng/mL) were added to 50 μL of plasma sample and centrifuged at 2,000×*g* for 5 min. The supernatants were filtered through a 0.20-μm filter and then analyzed by UPLC/ESI-MS. The column temperature was maintained at 65°C, and the standard and samples were separated using a gradient mobile phase consisting of acetonitrile (A) and 5 mM ammonium acetate (B) with a flow rate of 0.25 mL/min. The gradient method of analysis was 0–1.0 min, 50% A; 1.0–2.5 min, 70% A; 2.5–3.0 min, 84% A; 3.0–3.5 min, 95% A; and 3.5–4.0 min, 50% A. Peaks for internal standard and CsA were detected at retention times of 2.00 and 2.31 min, respectively. The pharmacokinetic parameters for CsA were calculated by means of noncompartmental methods using the WinNonlin program (Ver. 4.1, Pharsight Corporation, Mountain View, CA).

Tissue Distributions of CsA

The tissue accumulation of CsA in organs including the liver and kidney were estimated at T_{max} after oral administration of Neoral® (10 mg-CsA/kg) or intratracheal administration of nCsAm (100 μg-CsA/rat). Rats were sacrificed by obtaining blood from the descending aorta under temporary anesthesia with diethyl ether, and then the liver and kidney were carefully excised. The liver and kidney tissues were homogenized in 3 mL of saline using a Polytron PT 10-35 (Kinematica, Medfield, MA, USA). The homogenates were transferred into

test tubes. The tubes used for homogenizing had 1 mL of saline added to them for washing, and then the suspensions were transferred into stoppered test tubes. The stoppered test tubes had 4 mL of ethyl acetate added to them, followed by extraction on a shaker. After centrifugation (2,000×*g*, 5 min), the organic phases were collected into disposable glass tubes. This liquid–liquid extraction was repeated three times and all organic phases were pooled with each tissue and evaporated to dryness under a stream of nitrogen gas. The residues were dissolved in 1 mL of 70% acetonitrile. After centrifugation at 2,000×*g* for 5 min, 200 μL of acetonitrile and internal standard were added to 100 μL of samples. The supernatants were subjected to UPLC/ESI-MS analysis as described in the previous section.

Statistical Data Analysis

For statistical comparisons, one-way analysis of variance with pairwise comparison by Fisher's least significant difference procedure was used. A p value less than 0.05 was considered significant for all analyses.

RESULTS AND DISCUSSION

Physicochemical Properties of nCsAm

In the present study, nCsAm was prepared with the combination use of a flash nano-precipitation technique via MIVM and spray-drying. Although numerous pharmaceutical techniques based on bottom-up processes have been reported for manufacturing nano-particles, it has been challenging to control the nucleation and crystallization of drug compounds for the generation of uniform nano-particles (28). In the MIVM, intense mixing of the organic solvent solution containing the hydrophobic compound with water could induce a supersaturated state in times on the order of milliseconds to initiate rapid nano-precipitation, producing uniform nano-particles with a narrow size distribution (29,30). Lecithin was added to the sample solution as a dispersant, which coats the growing nanocrystals and stops aggregation to control the ultimate nanoparticle size. The hydrophobic tail of lipids adsorb onto the hydrophobic CsA surface and the hydrophilic head group extends into the external aqueous environment to provide both electrostatic and steric stabilization (31). The D_{50} of primary particles in the nano-suspension prepared with MIVM was 170.0 ± 5.4 nm before spray-drying. From the SEM observations, untreated CsA powder was composed of irregular shaped particles with diameters of 50–100 μm (Fig. 1a). The primary particle size of CsA nano-particles without mannitol was approximately 100–200 nm (Fig. 1b), which is consistent with the result of DLS analysis. In contrast, in nCsAm, CsA nano-particles dispersed in mannitol to form micron-sized aggregates during the spray-drying process (Fig. 1c). It has been reported that the addition of mannitol as a matrix former enhances the dissolution behavior of CsA due to improvements in dispersibility and wettability of CsA nano-particles (24). PXRD and DSC analysis for the evaluation of crystallinity demonstrated the amorphous state of CsA within the formulation (data not shown). From a physicochemical perspective, the amorphous form would be more readily soluble compared with the crystalline form due to its high energy state. The combination of the high energy amorphous solid form and the particles with nanometer size could lead to improvement of the dissolution behavior of CsA.

A drug must be adequately delivered to the affected area for efficacious therapy of respiratory diseases since its delivery might have major impact on the clinical outcomes, therapy cost, and medication compliance (32). Laser diffraction analysis with the dry system showed a volume median diameter of nCsAm around 1.3 μm and span value of 1.35 (Fig. 2a), suggesting well-controlled manufacturing of inhalable particles. The deposition pattern and aerodynamic behavior of inhaled nCsAm in the respiratory site were estimated using the NGI (Fig. 2b). As can be seen from the results of NGI analysis, nCsAm demonstrated a desirable inhalation profile as evidenced by the FPF value of 65.8% calculated with cut off diameter <5 μm. CsA was mainly deposited at stage 3 and 4 in NGI system, indicating the potential of nCsAm to reach the deep lung. The majority of aerosol particles with aerodynamic diameter of about 1–2 μm could be deposited in the peripheral regions of lung, if slowly and deeply inhaled (33). Although such fine particles are typically cohesive and likely to disperse poorly owing to their large surface area and low flowability, the nCsAm indicated a high emitted fraction and FPF value without the addition of coarse carrier particles. The surface morphology of the particle can significantly affect the aerosol performance of powders (34). In a previous report, surface roughness improved the dispersibility of powders (23) and the surface morphology of the nano-matrix particles in this study were similarly rough, as demonstrated by the SEM images (24). The nCsAm were found to be appropriate particles for effective delivery to the lung airways.

Anti-inflammatory Effect of nCsAm in Rat Model of Airway Inflammation

Inhalable formulations of CsA have provided potential therapeutic effects for lung transplant patients and corticosteroid-dependent asthma in previous reports (35–37). These therapeutic effects were accompanied by suppression of the serum levels of soluble IL-2 receptor and IL-2 receptor-binding $CD4^+$ T lymphocytes (38). These findings support the hypothesis that the therapeutic effect of CsA on airway inflammation is mediated by the inhibition of T cell activation. Local administration of CsA to the respiratory system can limit

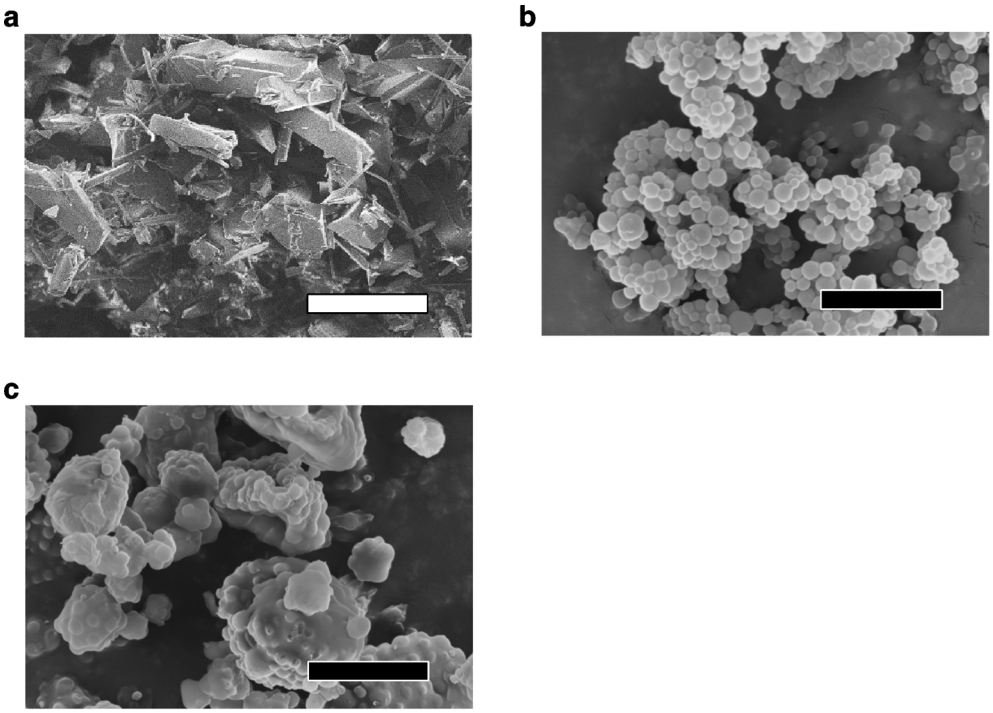

Fig. 1 Scanning electron microscopy of CsA samples. (**a**) untreated CsA, (**b**) CsA nanoparticles prepared by flash nanoprecipitation method without mannitol, and (**c**) nCsAm. *White* and *black bars* represent 50 μm and 2 μm, respectively.

systemic exposure and enhance the topical anti-inflammatory effect. To assess the therapeutic potential of nCsAm for airway inflammation, the anti-inflammatory effect was evaluated using OVA-sensitized asthma/COPD model rats (25). This OVA-sensitized animal has been widely used as an airway inflammation model, since repeated exposures of aerosolized OVA to actively immunized rats can induce the production of OVA-specific IgE, airway hyperresponsiveness, peribronchial inflammation, and an increase in BALF eosinophilia and neutrophilia (39). In the antigen-sensitized rat with intratracheal administration of the vehicle formulation, the total numbers of inflammatory cells and neutrophils in BALF significantly increased by ca. 5- and 10-fold, respectively (Table I). The OVA challenge in the airway induced pulmonary neutrophilia in rats, eventually injuring the epithelium and underlying basement membrane in pulmonary tissues (25). There were also slight increases in the numbers of eosinophils and macrophages after the antigen sensitization. These inflammatory cells could damage the pulmonary tissues due to the production of various cytokines and reactive oxygen free radicals (40). In contrast, there was significant suppression of the increase in total inflammatory cells and neutrophils recruitment in the nCsAm pre-treated group, showing 49.8% and 31.1% decreases, respectively. MPO is known to be the inflammatory cytokine released from neutrophils and macrophages driving inflammatory reactions and oxidative stress damage, and might be a potential target for some inflammatory diseases (41). The production of collagen within the lung tissue is a pathognomonic feature of fibrosis and remodeling of the lung tissues in COPD and chronic asthma (42). In vehicle-treated rats, OVA-induced increases in the MPO activity and production of collagen were observed due to the airway neutrophilia. In contrast, pretreatment of OVA-sensitized rats with nCsAm resulted in as much as 63.3% attenuation of MPO activity in BALF and 71.0% reduction of collagen production in the lung tissue (Fig. 3a and b). The results were also indicative of suppressing the neutrophilia in the airway system, suggesting the therapeutic potential of nCsAm for treatment of pulmonary inflammatory diseases.

Pharmacokinetic Study

In spite of the numerous reports about application of CsA to the treatment of respiratory inflammation, clinical and experimental trials through the oral route delivery have been limited due to concerns about various side-effects, including nephrotoxicity, hepatotoxicity, cardiotoxicity, and hypertension caused by high systemic exposure to the drug (9,43–45). An inhalable formulation could be a promising strategy to achieve site-specific delivery and thereby a safe and efficacious therapy for airway inflammation. A pharmacokinetic study on intratracheal and oral administration of CsA samples in rats was carried out to validate the advantage of inhalable CsA formulation. The present study demonstrated the plasma concentration-time profiles of CsA in rats after intratracheal administration of a therapeutic dose (0.1 mg-CsA/rat, *i.t.*) and oral administration of a toxic dose (10 mg-CsA/kg, *p.o.*) (46). The intratracheal nCsAm resulted in significantly lower systemic exposure to CsA compared with the oral CsA formulation with a nephrotoxic dose as evidenced by the C_{max} and

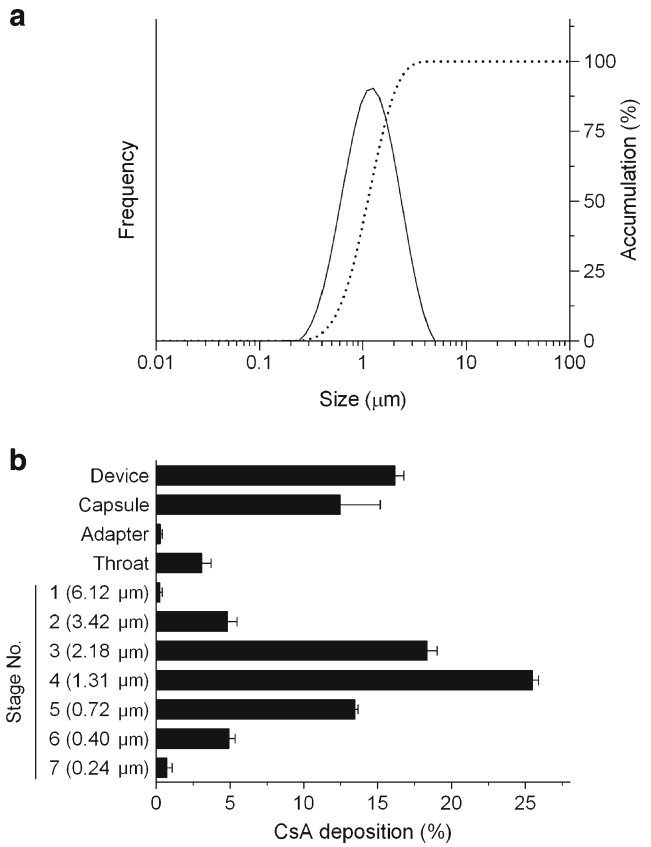

Fig. 2 *In vitro* inhalation properties of nCsAm. (**a**) Particle size distribution of nCsAm as determined by laser diffraction. The nCsAm was dispersed by dry air at 4 bars of pressure. *Dotted line* indicates the cumulative distribution of nCsAm particles. (**b**) *In vitro* aerosol performance evaluated by dispersing powder using an Aerolizer® inhaler through a Next Generation Impactor at an airflow rate of 100 L/min. The numbers in parentheses indicate aerodynamic cut off diameters for each stage.

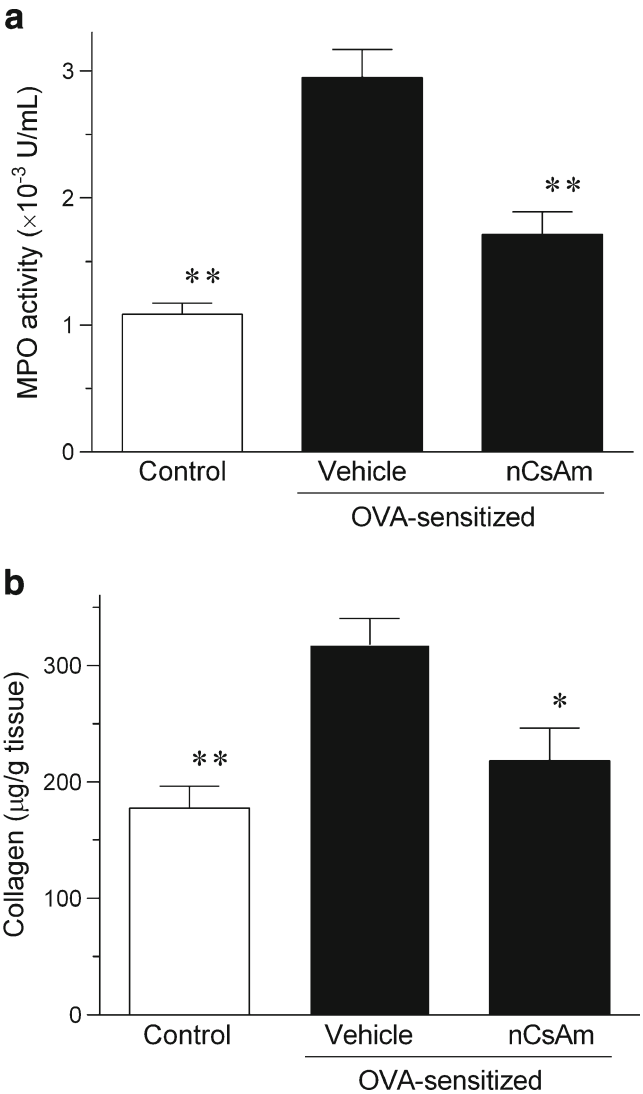

Fig. 3 Anti-inflammatory effects of nCsAm after intratracheal administration in rat model of acute airway inflammation. (**a**) MPO activities in BALF. Each value represents mean ± S.E. of 6 rats. (**b**) Collagen production in the lung tissue. Each value represents mean ± S.E. of 6 rats. ** $p < 0.01$, * $p < 0.05$ with respect to vehicle group.

AUC_{0-24} values of 225.5 ng/mL and 33,800 ng • h/mL, respectively (Fig. 4a and Table II). These observations would suggest that intratracheal nCsAm might be efficacious for avoidance of systemic side-effects because of reduced dosage amount upon topical administration. Further toxicity studies on nCsAm are needed to clarity the safety concern under chronic use. Local distributions of CsA in side-effects-related organs such as the kidney and liver were quantified at T_{max} after intratracheal and oral administration of CsA samples. Compared with orally-treated rats at a toxic dose, the tissue distributions of CsA within both the liver and kidney were lower in intratracheally-nCsAm-treated rats by 42- and 47-fold, respectively (Fig. 4b). The local renal accumulation of CsA could contribute significantly to chronic nephrotoxicity since the concentration of CsA is correlated with decline of renal function and increased histologic damage in the kidney (47). The CsA-induced acute renal dysfunction can be accompanied by the direct contraction of blood vessels and changes in various vasoconstrictor factors in the kidney (8,48,49). Excessive systemic exposure of CsA can induce free radical formation leading to acute renal and liver dysfunction

Table I Inflammatory Cell Recruitment in BALF

	Recoverable cells in BALF ($\times 10^5$ cells/mL)		
		OVA-sensitized	
	Control	Vehicle	nCsAm
Total cells	21.3 ± 2.9**	101.1 ± 14.9	50.4 ± 7.8*
Macrophages	13.2 ± 2.2	24.8 ± 2.4	24.5 ± 3.6
Neutrophils	7.4 ± 1.1**	73.5 ± 12.2	24.3 ± 4.9*
Eosinophils	0.8 ± 0.4	2.8 ± 0.5	1.6 ± 0.5

Data represent mean ± SE of 4 experiments

** $p < 0.01$, * $p < 0.05$ with respect to vehicle group

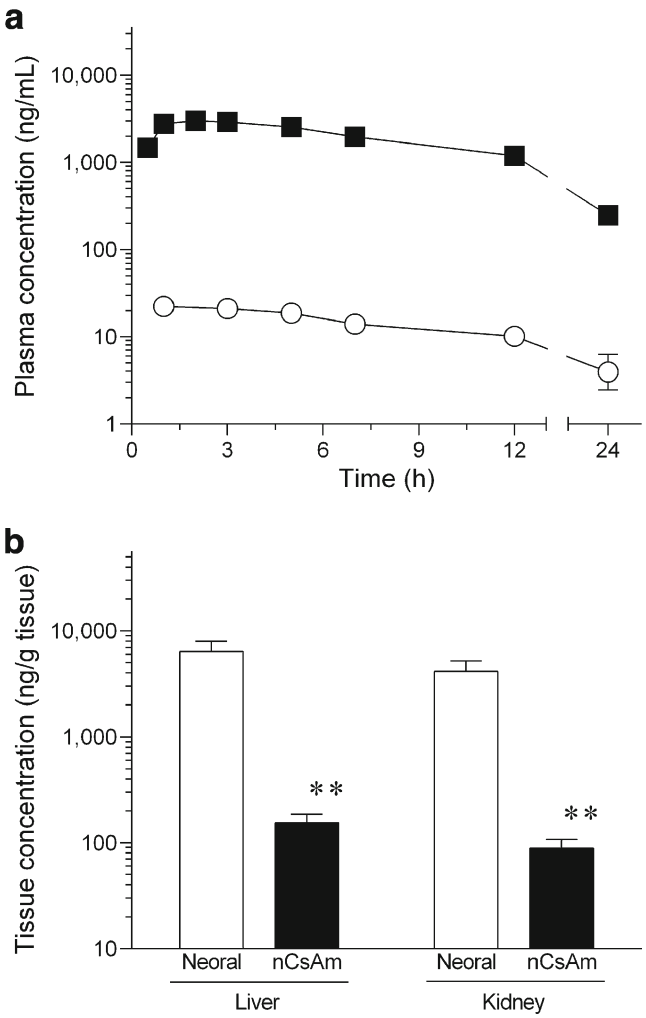

Fig. 4 Pharmacokinetic behavior of CsA samples after oral (10 mg-CsA/kg) and intratracheal (100 μg-CsA/rat) administration in rats. (**a**) Systemic exposure of CsA in plasma. ○, intratracheal nCsAm; and ■, oral Neoral®. Each value represents mean ± S.E. of 6 rats. (**b**) Tissue accumulation of CsA in the liver and kidney. Each value represents mean ± S.E. of 4–5 rats. ** $p < 0.01$ with respect to Neoral®-administrated group.

(45,49). Intratracheal nCsAm could reduce such systemic exposure as well as the limited local distributions of CsA, potentially leading to the avoidance of systemic side-effects. In a previous report, the systemic exposure after inhalation of a 20 mg dose was much lower than that achieved after administration of a 3 mg oral dose, suggesting a better safety margin with a higher therapeutic potential of inhalation (50). A number of inhalable CsA formulations have been developed to overcome the disadvantages, e.g., nebulizer formulation and metered-dose inhaler formulation (ADI628) (50,51). In previous clinical trials on inhalable CsA formulation, nebulized CsA exhibited beneficial effects in the lung transplant recipients in terms of pharmacokinetic behavior of CsA (14). Using inhalation system, adequate amount of CsA can be delivered to the pulmonary tissues of lung transplant patients without excessive systemic exposure of CsA (52). However, the liquid formulations contain organic solvents and surfactants such as ethanol, polyethylene glycol and propylene glycol as a solubilizer of CsA. These solvents are potential irritants, so that the liquid formulation of CsA aerosol is limited due to the risk of its local irritations. Therefore, DPI system like nCsAm would be a desirable option for the direct delivery of the drug to the respiratory systems, with no use of irritant ingredients.

It is possible to vary the pharmacokinetic behaviors of a concomitant drug owing to the inhibition of P-glycoprotein by systemic exposure of CsA. P-glycoprotein is expressed at the apical side of tubular epithelial cells and liver cells and is responsible for the excretion of various drugs. With respect to the metabolism, CsA undergoes extensive hepatic metabolism and can suppress the function of the cytochrome P450 system, leading to variations in the pharmacokinetic behaviors of the co-existing drugs that are substrates of P450, especially the 3A4 genotype. From these perspectives, excessive systemic exposure to CsA could induce higher blood concentrations of the concomitant drugs than single use, resulting in enhanced drug effects and subsequently adverse side-effects related to excessive drug exposure. The inhalable CsA formulation could also be beneficial in suppressing the risk of the drug-drug interaction due to the limited systemic exposure of CsA.

CONCLUSION

In the present study, nCsAm was successfully prepared with a flash nano-precipitation technology employing MIVM for inhalation therapy of airway inflammation. The *in vitro* inhalation properties and dispersibility of nCsAm were found to be efficient for desirable pulmonary delivery. Insufflated nCsAm suppressed antigen-evoked pulmonary inflammation in rats and minimize the systemic exposure and distribution to side-effect-related organs. These findings indicate that nanomatrix particles prepared with MIVM could be a viable

Table II Pharmacokinetic Parameters of CsA Formulations

	C_{max} (ng/mL)	T_{max} (h)	$T_{1/2}$ (h)	AUC_{0-24} (ng • h/mL)
nCsAm (0.1 mg-CsA/rat, *i.t.*)	38.2 ± 5.6	-	4.6 ± 1.2	256 ± 58.8
Neoral (10 mg-CsA/kg, *p.o.*)	3,190 ± 174	2.3 ± 0.6	5.6 ± 0.6	33,800 ± 2410

C_{max} maximum concentration, T_{max} time to maximum concentration, $T_{1/2}$ half life, AUC_{0-24} area under the curve of blood concentration *vs.* time from 0 to 24 h after administration. Data represent mean ± S.E. of 6 experiments

delivery option for the treatment of respiratory diseases with a better safety margin relative to orally administered drug.

ACKNOWLEDGMENTS AND DISCLOSURES

This work was supported in part by a Grant-in-Aid for Scientific Research (C) (No. 24590200; S. Onoue) from the Ministry of Education, Culture, Sports, Science and Technology, and a grant from the Takeda Science Foundation. This research was supported under Australian Research Council's *Discovery Projects* funding scheme (project number 120102778; H-K Chan). This work was also funded in part by the National Institutes of Health (Award No. 1RO1CA155061-1) which supported RKP.

REFERENCES

1. Venkataram S, Awni WM, Jordan K, Rahman YE. Pharmacokinetics of two alternative dosage forms for cyclosporine: liposomes and intralipid. J Pharm Sci. 1990;79(3):216–9.
2. Sajjadi H, Soheilian M, Ahmadieh H, Hassanein K, Parvin M, Azarmina M, *et al.* Low dose cyclosporin-A therapy in Behcet's disease. J Ocul Pharmacol. 1994;10(3):553–60.
3. Thomson AW, Neild GH. Cyclosporin: use outside transplantation. BMJ. 1991;302(6767):4–5.
4. Matsuda Y, Chen F, Miyata H, Date H. Once-daily oral administration of cyclosporine in a lung transplant patient with a history of renal toxicity of calcineurin inhibitors. Interact Cardiovasc Thorac Surg. 2014;19(1):171–3.
5. Bousquet J, Jeffery PK, Busse WW, Johnson M, Vignola AM. Asthma. From bronchoconstriction to airways inflammation and remodeling. Am J Respir Crit Care Med. 2000;161(5):1720–45.
6. Sato H, Ogawa K, Kojo Y, Kawabata Y, Mizumoto T, Yamada S, *et al.* Development of cyclosporine A-loaded dry-emulsion formulation using highly purified glycerol monooleate for safe inhalation therapy. Int J Pharm. 2013;448(1):282–9.
7. Onoue S, Sato H, Kawabata Y, Mizumoto T, Hashimoto N, Yamada S. In vitro and in vivo characterization on amorphous solid dispersion of cyclosporine A for inhalation therapy. J Control Release. 2009;138(1):16–23.
8. Bobadilla NA, Gamba G. New insights into the pathophysiology of cyclosporine nephrotoxicity: a role of aldosterone. Am J Physiol Renal Physiol. 2007;293(1):F2–9.
9. Rezzani R. Cyclosporine A, and adverse effects on organs: histochemical studies. Prog Histochem Cytochem. 2004;39(2):85–128.
10. Ismailos G, Reppas C, Dressman JB, Macheras P. Unusual solubility behaviour of cyclosporin A in aqueous media. J Pharm Pharmacol. 1991;43(4):287–9.
11. Courrier HM, Butz N, Vandamme TF. Pulmonary drug delivery systems: recent developments and prospects. Crit Rev Ther Drug Carrier Syst. 2002;19(4–5):425–98.
12. Charnick SB, Yu Z, Athill LV, Karara AH, Tse FL, Lau DT. Pharmacokinetics of SDZ 64-412, a novel antiasthmatic agent, following intravenous, oral, and inhalation dosing in the rat. Biopharm Drug Dispos. 1994;15(4):317–27.
13. Onoue S, Aoki Y, Kawabata Y, Matsui T, Yamamoto K, Sato H, *et al.* Development of inhalable nanocrystalline solid dispersion of tranilast for airway inflammatory diseases. J Pharm Sci. 2011;100(2):622–33.
14. Iacono AT, Johnson BA, Grgurich WF, Youssef JG, Corcoran TE, Seiler DA, *et al.* A randomized trial of inhaled cyclosporine in lung-transplant recipients. N Engl J Med. 2006;354(2):141–50.
15. Behr J, Zimmermann G, Baumgartner R, Leuchte H, Neurohr C, Brand P, *et al.* Munich lung transplant G. lung deposition of a liposomal cyclosporine A inhalation solution in patients after lung transplantation. J Aerosol Med Pulm Drug Deliv. 2009;22(2):121–30.
16. Crompton GK. Dry powder inhalers: advantages and limitations. J Aerosol Med. 1991;4(3):151–6.
17. Frijlink HW, De Boer AH. Dry powder inhalers for pulmonary drug delivery. Expert Opin Drug Deliv. 2004;1(1):67–86.
18. Clarke SW, Pavia D. Lung mucus production and mucociliary clearance: methods of assessment. Br J Clin Pharmacol. 1980;9(6):537–46.
19. Lehnert BE, Valdez YE, Tietjen GL. Alveolar macrophage-particle relationships during lung clearance. Am J Respir Cell Mol Biol. 1989;1(2):145–54.
20. Onoue S, Misaka S, Kawabata Y, Yamada S. New treatments for chronic obstructive pulmonary disease and viable formulation/device options for inhalation therapy. Expert Opin Drug Deliv. 2009;6(8):793–811.
21. Wu X, Zhang W, Hayes Jr D, Mansour HM. Physicochemical characterization and aerosol dispersion performance of organic solution advanced spray-dried cyclosporine A multifunctional particles for dry powder inhalation aerosol delivery. Int J Nanomedicine. 2013;8:1269–83.
22. Zijlstra GS, Rijkeboer M, Jan van Drooge D, Sutter M, Jiskoot W, van de Weert M, *et al.* Characterization of a cyclosporine solid dispersion for inhalation. AAPS J. 2007;9(2):E190–9.
23. Kwok PC, Tunsirikongkon A, Glover W, Chan HK. Formation of protein nano-matrix particles with controlled surface architecture for respiratory drug delivery. Pharm Res. 2011;28(4):788–96.
24. Yamasaki K, Kwok PC, Fukushige K, Prud'homme RK, Chan HK. Enhanced dissolution of inhalable cyclosporine nano-matrix particles with mannitol as matrix former. Int J Pharm. 2011;420(1):34–42.
25. Misaka S, Sato H, Yamauchi Y, Onoue S, Yamada S. Novel dry powder formulation of ovalbumin for development of COPD-like animal model: physicochemical characterization and biomarker profiling in rats. Eur J Pharm Sci. 2009;37(3–4):469–76.
26. Misaka S, Aoki Y, Karaki S, Kuwahara A, Mizumoto T, Onoue S, *et al.* Inhalable powder formulation of a stabilized vasoactive intestinal peptide (VIP) derivative: anti-inflammatory effect in experimental asthmatic rats. Peptides. 2010;31(1):72–8.
27. Aoki Y, Kojo Y, Yamada S, Onoue S. Respirable dry powder formulation of bleomycin for developing a pulmonary fibrosis animal model. J Pharm Sci. 2012;101(6):2074–81.
28. D'Addio SM, Prud'homme RK. Controlling drug nanoparticle formation by rapid precipitation. Adv Drug Deliv Rev. 2011;63(6):417–26.
29. Pinkerton NM, Gindy ME, Calero-Ddel CV, Wolfson T, Pagels RF, Adler D, *et al.* Single-step assembly of multimodal imaging nanocarriers: MRI and long-wavelength fluorescence imaging. Adv Healthcare Mater. 2015;4(9):1376–85.
30. Gindy ME, Panagiotopoulos AZ, Prud'homme RK. Composite block copolymer stabilized nanoparticles: simultaneous encapsulation of organic actives and inorganic nanostructures. Langmuir. 2008;24(1):83–90.
31. Gajra B, Dalwadi C, Patel R. Formulation and optimization of itraconazole polymeric lipid hybrid nanoparticles (Lipomer) using box behnken design. Daru. 2015;23:3.
32. Patton JS, Byron PR. Inhaling medicines: delivering drugs to the body through the lungs. Nat Rev Drug Discov. 2007;6(1):67–74.

33. Byron PR. Prediction of drug residence times in regions of the human respiratory tract following aerosol inhalation. J Pharm Sci. 1986;75(5):433–8.
34. Chan HK. What is the role of particle morphology in pharmaceutical powder aerosols? Expert Opin Drug Deliv. 2008;5(8):909–14.
35. Alexander AG, Barnes NC, Kay AB. Trial of cyclosporin in corticosteroid-dependent chronic severe asthma. Lancet. 1992;339(8789):324–8.
36. Groves S, Galazka M, Johnson B, Corcoran T, Verceles A, Britt E, *et al.* Inhaled cyclosporine and pulmonary function in lung transplant recipients. J Aerosol Med Pulm Drug Deliv. 2010;23(1):31–9.
37. Dykewicz MS. Newer and alternative non-steroidal treatments for asthmatic inflammation. Allergy Asthma Proc. 2001;22(1):11–5.
38. Underwood SL, McMillan S, Reeves R, Hunt J, Brealey CJ, Webber S, *et al.* Effects of cyclosporin A administered into the airways against antigen-induced airway inflammation and hyperreactivity in the rat. Eur J Pharmacol. 2001;420(2–3):165–73.
39. Brusselle G, Kips J, Joos G, Bluethmann H, Pauwels R. Allergen-induced airway inflammation and bronchial responsiveness in wild-type and interleukin-4-deficient mice. Am J Respir Cell Mol Biol. 1995;12(3):254–9.
40. Barnes PJ. Mediators of chronic obstructive pulmonary disease. Pharmacol Rev. 2004;56(4):515–48.
41. O'Donnell C, Newbold P, White P, Thong B, Stone H, Stockley RA. 3-Chlorotyrosine in sputum of COPD patients: relationship with airway inflammation. COPD. 2010;7(6):411–7.
42. Postma DS, Timens W. Remodeling in asthma and chronic obstructive pulmonary disease. Proc Am Thorac Soc. 2006;3(5):434–9.
43. Ingawale DK, Mandlik SK, Naik SR. Models of hepatotoxicity and the underlying cellular, biochemical and immunological mechanism(s): a critical discussion. Environ Toxicol Pharmacol. 2014;37(1):118–33.
44. Nash EF, Stephenson A, Helm EJ, Durie PR, Tullis E, Singer LG, *et al.* Impact of lung transplantation on serum lipids in adults with cystic fibrosis. J Heart Lung Transplant. 2011;30(2):188–93.
45. El-Gowelli HM, El-Mas MM. Central modulation of cyclosporine-induced hypertension. Naunyn Schmiedebergs Arch Pharmacol. 2015;388(3):351–61.
46. Bohdanecka M, Schuck O, Chadimova M, Sedivy J, Glagolicova A, Skibova J, *et al.* Nephrotoxicity of cyclosporin A in hereditary hypertriglyceridemic rats. Physiol Res. 1999;48(6):437–43.
47. Podder H, Stepkowski SM, Napoli KL, Clark J, Verani RR, Chou TC, *et al.* Pharmacokinetic interactions augment toxicities of sirolimus/cyclosporine combinations. J Am Soc Nephrol. 2001;12(5):1059–71.
48. Olyaei AJ, de Mattos AM, Bennett WM. Nephrotoxicity of immunosuppressive drugs: new insight and preventive strategies. Curr Opin Crit Care. 2001;7(6):384–9.
49. Naesens M, Kuypers DR, Sarwal M. Calcineurin inhibitor nephrotoxicity. Clin J Am Soc Nephrol. 2009;4(2):481–508.
50. Rohatagi S, Calic F, Harding N, Ozoux ML, Bouriot JP, Kirkesseli S, *et al.* Pharmacokinetics, pharmacodynamics, and safety of inhaled cyclosporin A (ADI628) after single and repeated administration in healthy male and female subjects and asthmatic patients. J Clin Pharmacol. 2000;40(11):1211–26.
51. Iacono AT, Corcoran TE, Griffith BP, Grgurich WF, Smith DA, Zeevi A, *et al.* Aerosol cyclosporin therapy in lung transplant recipients with bronchiolitis obliterans. Eur Respir J. 2004;23(3):384–90.
52. Corcoran TE, Niven R, Verret W, Dilly S, Johnson BA. Lung deposition and pharmacokinetics of nebulized cyclosporine in lung transplant patients. J Aerosol Med Pulm Drug Deliv. 2014;27(3):178–84.